APPLIED AND ENVIRONMENTAL MICROBIOLOGY, Apr. 1992, p. 1142–1152
0099-2240/92/041142-11$02.00/0

Vol. 58, No. 4

Differential Bioavailability of Soil-Sorbed Naphthalene to Two Bacterial Species

WILLIAM F. GUERIN* AND STEPHEN A. BOYD

Department of Crop and Soil Science, Michigan State University, East Lansing, Michigan 48824-1325

Received 21 October 1991/Accepted 31 January 1992

Prediction of the fate of hydrophobic organic contaminants in soils is complicated by the competing processes of sorption and biodegradation. To test the hypothesis that sorbed naphthalene is unavailable to degradative microorganisms, we developed a simple kinetic method to examine the rates and extents of naphthalene degradation in soil-free and soil-containing systems in a comparison of two bacterial species. The method is predicated on the first-order dependence of the initial mineralization rate on the naphthalene concentration when the latter is below the Michaelis-Menten half-saturation constant (K_m) for naphthalene for the organism under study. Rates and extents of mineralization were estimated by nonlinear regression analysis of data by using both a simple first-order model and a three-parameter, coupled degradation-desorption model described for the first time here. Bioavailability assays with two bacterial species (*Pseudomonas putida* ATCC 17484 and a gram-negative soil isolate, designated NP-Alk) gave dramatically different results. For NP-Alk, sorption limited both the rate and extent of naphthalene mineralization, in accordance with values predicted on the basis of the equilibrium aqueous-phase naphthalene concentrations. For strain 17484, both the rates and extents of naphthalene mineralization exceeded the predicted values and resulted in enhanced rates of naphthalene desorption from the soils. We conclude that there are important organism-specific properties which make generalizations regarding the bioavailability of sorbed substrates inappropriate.

Naphthalene is one of a large number of nonionic organic contaminants (NOCs) found in soils, sediments, and surface and groundwaters. It is a minor component of refined petroleum products, is abundant in coal and coal tar (18), and is important in chemical manufacturing. Its environmental fate is governed by its moderate solubility (31.7 mg liter^{-1}; 23), vapor pressure (0.23 mm Hg; 25), and sorption to particulates (log K_{oc} = 2.74; 1), as well as its susceptibility to degradation by a diversity of bacteria. Individually, the various fate processes have been studied in some detail; however, little is known about the interactions of these processes. Specifically, the influence of sorption on naphthalene biodegradation is poorly understood for this and other NOCs. From a practical standpoint, rendering organic contaminants unavailable to potential microbial degraders by sorption to soil could seriously impede efforts to bioremediate contaminated sites. From a more basic standpoint, the influences of surfaces on microbial activities and ways in which specific attributes of bacteria (such as attachment, chemotaxis, and motility) affect their ability to utilize sorbed substrates are long-standing questions in microbial physiological ecology (9, 22, 35, 39).

For NOCs, sorption isotherms (plots of the NOC concentration in the sorbed state versus its equilibrium aqueous-phase concentration) are characteristically linear over broad concentration ranges, with slopes (partition coefficients [K_ps]) increasing with increasing organic carbon content of the sorbent. Normalization of the partition coefficients to the fractional organic carbon contents (f_{oc}s) of the sorbents yield convergent K_{oc} ($=K_p/f_{oc}$) values related to the aqueous solubility of the sorbate. NOC sorption can therefore be viewed as a partitioning process in which the particulate organic matter acts as an organic solvent phase (7). In contrast to ionic organic contaminants, NOCs show little tendency to adsorb to mineral surfaces which are polar and/or electrostatically charged and therefore strongly hydrated. The preferential adsorption of water by minerals in soil-water systems prohibits NOCs from interacting with these surfaces.

NOC sorption is generally regarded as a very rapid process, with apparent equilibrium attained in 24 h or less. However, as equilibration times increase, more aggressive extraction methods are often required to remove NOCs from soils and sediments (15, 34). Desorption of bound NOCs often exhibits hysteresis in which some of the sorbed material desorbs slowly or appears to be irreversibly bound. To explain these kinetic observations, a two-compartment (mass transfer) model of NOC sorption to soils and sediments has been developed by Karickhoff (15). According to this conceptual model, sorbed NOCs partition increasingly from a labile to a nonlabile phase with increasing equilibration time and decreasing solubility of the sorbate. Other mechanistically based models have used intraparticle diffusion (3, 38) and intraorganic matter diffusion (6) to provide an explanation for the observed phenomena.

The influence of sorption on the biodegradation of NOCs has been the subject of much speculation but little definitive experimentation. Sorption is generally thought to limit the availability of organic compounds, although the few published studies in this area (10, 16, 24, 27, 31, 33, 34, 36) have examined a wide assortment of organic compounds and a limited number and variety of degradative organisms and arrived at alternate conclusions regarding whether or not sorbed compounds are available to microbial degraders. These inconsistencies are attributable to differences in the chemical properties of the sorbate, the nature of the sorbent, the mechanism of sorption, the time allowed for sorbate-sorbent equilibration, and the properties of the degradative organisms. Thus, diquat (a dipyridylium cationic herbicide)

* Corresponding author.

was available to microbial degraders when sorbed to the external exchange sites of a nonexpanding clay mineral (kaolonite) and unavailable when bound in the interlayers of the expanding clay mineral montmorillonite (36). In settled stream sediments, cationic surfactants were also unavailable, whereas phenol (a nonionic compound at neutral pH) was available (31). Adsorption of low-molecular-weight organic acids to hydroxyapatite (a positively charged mineral) decreased their availability (10). Sorbed (2,4-dichlorophenoxy)acetic acid (2,4-D) was completely unavailable to a *Flavobacterium* sp., while dissolved 2,4-D was degraded by free-living and attached bacteria with nearly equal efficiencies (24). Protein (bovine serum albumin), because of its extensive electrostatic interactions with natural sorbents, was unavailable to nonattached microbial degraders but was readily degraded by attached bacteria, while a readily desorbable dipeptide was more efficiently degraded by free-living bacteria (11). When freshly added to field soils, ethylene dibromide was completely utilizable by indigenous bacteria. However, residual ethylene dibromide in field-aged soils was completely unavailable (34). These studies serve to illustrate the complexities inherent in studies in which both physicochemical and microbiological factors are at play.

In this report, we describe the development and application of a simple, yet powerful kinetic method to test the hypothesis that soil-sorbed naphthalene is unavailable to microbial degraders. We also introduce a new kinetic model which describes the coupled processes of mineralization and desorption of bound naphthalene and provides information about ways in which microorganisms may influence the rate of naphthalene desorption from soils.

MATERIALS AND METHODS

Soils. Four surface soils were collected from agricultural settings in southern Michigan. Soils were air dried and ground to pass a 2-mm sieve. Soils were characterized with respect to cation-exchange capacity (26), organic carbon content (Huffman Laboratories, Golden, Colo.), and particle size distribution by the hydrometer method (12).

Naphthalene sorption isotherms were performed for each soil by the batch method. Briefly, dried soil (1 g) was weighed into 25-ml glass centrifuge tubes. Solutions containing various concentrations of naphthalene were added to the tubes. These solutions consisted of a fixed volume (5 ml) of a [^{14}C]naphthalene solution (in phosphate-buffered saline [PBS], 8.5 g of NaCl, 0.3 g of KH_2PO_4, 0.6 g of Na_2HPO_4 per liter of distilled water, pH 7.0) of known activity, variable volumes of an unlabeled naphthalene solution (in PBS) of known concentration (determined by A_{277} measurement), and sufficient PBS to attain a total solution volume of 26 ml. A 1-ml portion of each solution was added to 7.5 ml of scintillation fluid to estimate the initial activity; the remaining 25 ml was added to centrifuge tubes containing soil or control tubes containing no soil. These were sealed with foil liners inside the Teflon-lined screw-on caps and shaken overnight. Equilibration was found to be complete after this time. Tubes were centrifuged (12,100 × *g*, 15 min; Sorvall RC5C refrigerated centrifuge), aliquots of the supernatants were withdrawn, and the activity of [^{14}C]naphthalene was determined by liquid scintillation counting (Packard 1500 Tri-Carb Liquid Scintillation Analyzer). Counts were converted to disintegrations per minute by external-standard quench correction, and the concentration of naphthalene in the aqueous phase was determined. The soil concentration was determined by difference. Recovery in soil-free controls averaged >95%. From the highly linear sorption isotherms, the slopes (naphthalene K_ps) were determined by linear regression. Normalization of K_ps to the fractional organic carbon contents of the soils yielded K_{oc} values.

Bacterial cultures. Two naphthalene-degrading isolates were used in these studies. *Pseudomonas putida* 17484 was obtained from the American Type Culture Collection. Aspects of the biochemistry (4) and genetics (8, 29) of naphthalene degradation by this organism have been described previously. A second isolate, designated NP-Alk, was isolated from a naphthalene-degrading enrichment originating from petroleum-contaminated soil. This organism was isolated by treating an aliquot of the active enrichment culture with alkaline citrate for 10 min, neutralizing the treated aliquot by addition of PBS, and plating the neutralized soil-bacterium suspension on a minimal agar medium (high-buffer agar; see below). Naphthalene, as the sole carbon and energy source, was supplied as a solid inside the covers of inverted plates sealed with Parafilm. Robust single colonies were streaked to purification on nutrient agar plates. Examination of NP-Alk by phase-contrast microscopy and transmission electron microscopy showed it to be, like strain 17484, a motile, gram-negative organism. A more complete description of this organism is in preparation.

Growth media. Cells were grown in liquid medium to which naphthalene was added as a concentrated stock solution in acetone (0.2 g ml^{-1}) to a final concentration of 200 mg liter^{-1}. The liquid medium (high-buffer broth) consisted of (per liter of distilled water) 2.0 g of NaCl, 3.0 g of $(NH_4)_2HPO_4$, 1.2 g of KH_2PO_4, 3 mg of $MgSO_4$, 1 ml of ferric quinate (0.27 g of $FeCl_3 \cdot 6H_2O$, 0.19 g of quinic acid per 100 ml of distilled water), 1 ml of a trace element solution (30), and 1 ml of a vitamin solution (37), pH 7.0. Cells were cultured with shaking (150 rpm) at room temperature in 500-ml sidearm flasks. Growth was monitored with a Spectronic 88 spectrophotometer by measuring the A_{600}. High-buffer agar medium was high-buffer broth to which 1.5% agar had been added.

Nutrient broth (Difco) was used at one-half of the recommended concentration in distilled water. Nutrient agar plates were made by addition of 1.5% agar to nutrient broth.

Naphthalene degradation studies. Organisms were characterized as to mode and extent of naphthalene degradation by several methods. Filtered (0.2-μm Millex; Millipore Corp., Bedford Mass.) supernatant fluids (12,100 × *g*, 10 min) of naphthalene-degrading cultures were analyzed by high-performance liquid chromatography (HPLC; Waters 6000A Solvent Delivery System, 720 System Controller, and 730 Data Module; Brownlee Spheri-5 C_{18} column [4.6 by 220 mm]) with linear-gradient elution (0 to 100% acetonitrile [Mallinckrodt] at 5% min^{-1} with a starting solvent of 100% H_2O [HPLC grade; Baker] adjusted to pH 2.75 with H_3PO_4 [Mallinckrodt; reagent grade]) at a constant flow rate of 1 ml min^{-1} by using the direct-injection procedure (14). Detection was by UV absorbance (277 nm; Waters 480 LC spectrophotometer) or liquid scintillation counting of 1-ml aliquots of labeled analyte collected from the column effluent. For identification, chromatogram peak retention times were compared to those of authentic compounds known to be intermediates in the naphthalene degradation pathway (17).

Supernatant fluids were also analyzed for naphthalene intermediates by a colorimetric method described previously (14), by reaction with ferric nitrate for salicylate analysis, and, for NP-Alk, by gas chromatography-mass spectrometry analysis of concentrated (under N_2) ethyl acetate extracts of acidified (pH 2) supernatant fluids.

[^{14}C]naphthalene mineralization assays. Mineralization of ^{14}C-labeled naphthalene (10.3 mCi mmol^{-1}, 98% radiochemical purity; Sigma) was determined in batch assays. Mineralization media were prepared by addition of ^{14}C-labeled naphthalene stock solution (in acetone) and unlabeled naphthalene stock solution to PBS (0.2 μm filtered) in a sterile dispenser flask to result in solutions with a total activity of approximately 5,000 dpm ml^{-1} and total naphthalene concentrations ranging from 40 to 100 ng ml^{-1}. The naphthalene stock solution was prepared by heating a particulate naphthalene suspension (in PBS) to 95°C, cooling it while stirring it, and filtering it through a 0.2-μm Nuclepore filter. Medium was dispensed aseptically, by using a glass volumetric 25-ml dispenser head to minimize volatilization losses, into sterile 155-ml serum vials with or without soil presterilized by autoclaving after being left wet overnight to promote spore germination. Total initial activity (and concentration) was determined by averaging counts of 1-ml aliquots of the aqueous naphthalene solution sampled before, during, and after dispensation. Total aqueous volumes were 75 to 78 ml. Vials were crimp sealed with Teflon-faced septa. Soil slurries were equilibrated by machine shaking overnight, followed by periodic shaking by hand, for periods ranging from days to months before inoculation.

To initiate mineralization assays, media were inoculated with 750 μl of washed (with PBS) early-stationary-phase suspensions of naphthalene-grown cells to a final density of 10^7 to 10^8 ml^{-1}. At precisely timed intervals, and after settling of large soil particles, duplicate aliquots containing equal proportions of headspace and liquid suspension were withdrawn by syringe and transferred to sealed tubes containing 1 ml of 2 N HCl. Evolved $^{14}CO_2$ was trapped on pleated filter paper saturated with 1 N KOH and suspended from the tube stopper inside a plastic cup. After overnight degassing, filter papers were transferred to scintillation vials containing 7.5 ml of scintillation fluid along with 5 ml of 95% ethanol, used to rinse the plastic cup. After several hours in the dark to allow chemiluminescence to subside, samples were analyzed for $^{14}CO_2$ as described above.

Models of mineralization kinetics. Mineralization data (expressed as the percentage [P] of the initial activity converted to $^{14}CO_2$ as a function of time [t]) were fitted to a first-order production equation of the following form:

$$P = P_{max}(1 - e^{-kt}) \quad (1)$$

Nonlinear regression analysis (SYSTAT) was used to estimate the parameters P_{max} (maximal percentage mineralized) and k (first-order rate constant). The rate constant, k (minute^{-1}), was normalized to P_{max} and the initial naphthalene concentration (in nanograms milliliter^{-1}) to obtain initial mineralization rates (in nanograms milliliter^{-1} minute^{-1}). The parameters derived from this model accurately describe the mineralization kinetics of nonsorbed naphthalene in systems under equilibrium (instantaneous sorption and/or desorption) and pseudoequilibrium (desorption rates much slower than degradation rates) conditions. They are also minimal estimates of degradation, since ^{14}C-labeled naphthalene conversion to biomass is not accounted for.

Mineralization data were also fitted to an alternative first-order model based on one which describes the progress of an enzyme-catalyzed reaction (p) over time (t) following addition of a slowly binding inhibitor (21):

$$p = v_2t + [(v_1 - v_2)(1 - e^{-kt})]/k \quad (2)$$

Here, the reaction rate changes from that prior to inhibitor binding, v_1, to a new inhibited rate, v_2, with a first-order rate constant, k. This and similar models (5) provide fits to biphasic curves in which an exponential phase is followed and accompanied by a linear phase of reaction. In the case of enzyme inhibition, the presence of the inhibitor acts to underestimate the kinetics of the first-order reaction, giving rise to the term $v_1 - v_2$. In our application, a first-order exponential phase of dissolved naphthalene mineralization is followed and accompanied by a linear phase of mineralization of desorbing naphthalene. Since desorption makes a positive contribution to (overestimates) the exponential phase of dissolved naphthalene mineralization (as soon as the sorptive equilibrium is upset by utilization of dissolved or otherwise accessible naphthalene), we have modified the above-described model simply by changing the sign of the rate term as follows:

$$P = v_2t + [(v_1 + v_2)(1 - e^{-kt})]/k \quad (3)$$

Here, v_1 represents the initial reaction rate (percent minute^{-1}), which when normalized to the initial naphthalene concentration (nanograms milliliter^{-1}), gives initial mineralization rates (nanograms milliliter^{-1} minute^{-1}) directly comparable to those derived by using the first-order model (equation 1). The asymptote of the exponential phase is defined by v_1/k (percent), and is the equivalent of P_{max} (equation 1). The parameter v_2 represents the mineralization rate resulting from desorption of bound naphthalene and is related to the kinetics of naphthalene desorption. The parameter k (minute^{-1}) is the first-order rate constant, and P is the percentage of naphthalene mineralized as a function of time, t. We have found empirically that this simple three-parameter model, in which mineralization of desorbing naphthalene is described by a linear-rate term (v_2t), provides excellent fits to our experimental data. Here, we present data which validate the use of this model as a first approximation of the kinetics of sorbed substrate mineralization under equilibrium and nonequilibrium conditions.

Assessment of bioavailability. At concentrations below the half-saturation constant (K_m) for naphthalene mineralization, mineralization rates are directly proportional to substrate concentration (2, 19). Assuming that sorbed naphthalene is unavailable to microbial degraders, increasing the soil-solution ratio and concomitantly decreasing the equilibrium aqueous-phase naphthalene concentration should result in proportionate decreases in initial mineralization rates ($k[P_{max}]$ [nanograms of naphthalene milliliter^{-1}] or v_1 [nanograms of naphthalene milliliter^{-1}]). Furthermore, data for mineralization rates versus the equilibrium aqueous-phase naphthalene concentration should fall on a straight line connecting a soil-free datum point with the origin. Deviation from this line would indicate that the cells experience a higher (deviations above the line) or lower (deviations below the line) naphthalene concentration than that which is present in the aqueous phase.

Although incorporated into mineralization rate calculations by using the simple first-order model, P_{max} is independent of the parameter k (28). Similar analyses of P_{max} data thus provide additional information on the influence of sorption on the extent of mineralization. Decreases in P_{max} below the soil-free control value would be expected if sorption limited the extent of mineralization. P_{max} values falling on a theoretical line connecting the soil-free control P_{max} value to the origin define the condition in which only dissolved naphthalene is utilized and desorption is slow relative to the time course of the assay. Upward deviations from the line indicate an increased rate of desorption and/or accessibility of sorbed naphthalene to the bacteria. With the

TABLE 1. Physical and chemical properties of the soils used in this study

Soil series	Order	% OC[a]	CEC[b]	% Sand	% Silt	% Clay	K_p[c]	log K_{oc}[d]
Capac	Alfisol	3.46	12.2	44	36	20	12.51	2.56
Colwood	Mollisol	5.36	21.6	41	35	24	28.93	2.73
Oshtemo	Alfisol	0.76	5.6	69	15	16	4.56	2.78
Schoolcraft	Mollisol	1.84	8.0	39	42	19	8.07	2.64

[a] Percent organic carbon (dry weight).
[b] Cation exchange capacity (milliequivalents/100 g^{-1}).
[c] Naphthalene partition coefficient (milliliters $gram^{-1}$).
[d] Log of the organic carbon-normalized partition coefficient ($K_{oc} = K_p/f_{oc}$).

coupled degradation-desorption model (equation 3), the extent of the exponential reaction is given by v_1/k (percent). This value describes the size of the immediately accessible naphthalene pool. If sorbed naphthalene is unavailable and desorbs slowly relative to the biodegradation rate, v_1/k values should be proportional to the equilibrium aqueous-phase naphthalene concentration and fall on a theoretical line connecting the soil-free control value to the origin.

RESULTS

Table 1 shows the characteristics of the soils used in this study. Organic carbon ranged from 0.76% for Oshtemo soil to 5.36% for Colwood soil. Naphthalene sorption to all soils resulted in highly linear isotherms. As expected, the measured naphthalene K_ps increased with increasing organic carbon, ranging from 4.56 to 28.93. Logarithms of the partition coefficients normalized to the fractional organic carbon contents of the soils (average log K_{oc} = 2.68) agreed well with the literature value of 2.74 (1). Knowing the partition coefficients for the soils, it is possible to calculate the concentrations of naphthalene in the sorbed and dissolved phases at equilibrium when the mass of added naphthalene and soil-solution ratios are known.

Both of the organisms used in this study were found to carry out complete and coordinate mineralization of naphthalene without accumulating metabolic intermediates. Analysis of culture supernatant fluids during growth of cultures on naphthalene showed insignificant amounts of UV-absorbing, Folin- or $Fe(NO_3)_3$-reactive intermediates. Analysis of NP-Alk culture extracts by gas chromatography-mass spectrometry confirmed this result. Liquid scintillation counting of HPLC eluent fractions from supernatant fluids of ^{14}C-labeled naphthalene-grown cells also showed the absence of significant quantities of labeled metabolites. These results support the use of $^{14}CO_2$ evolution from ^{14}C-labeled naphthalene as a reliable index of biodegradation and indicate that bioavailability assays are not confounded by production of metabolites which would partition differently from the parent compound between the sorbed and aqueous phases.

Mineralization rates were measured over a range of initial naphthalene concentrations (20 to 555 ng ml^{-1}) for both organisms. Treating stationary, nongrowing cells as enzymes, mineralization rate and naphthalene concentration data were fitted to the Michaelis-Menten equation by nonlinear regression analysis (21, 28) to derive estimates of K_m (in nanograms $milliliter^{-1}$) for naphthalene and V_{max} (in nanograms $cell^{-1}$ $minute^{-1}$). The K_m for strain 17484 mineralizing naphthalene (211 ng ml^{-1}) was about twice that for Np-Alk (91 ng ml^{-1}), which also showed a lower V_{max} (5.32×10^{-7} versus 7.83×10^{-7} ng $cell^{-1}$ min^{-1}). Kinetic constants determined by nonlinear regression agreed well with values obtained by linear regression of linearized data (i.e., Lineweaver-Burke plots). For the latter, r^2 values of 0.99 or better were obtained for both organisms. To ensure a linear response between mineralization rates and naphthalene concentrations in bioavailability experiments, initial naphthalene concentrations were generally less than 0.5 times the K_m (20). At the cell densities used in the bioavailability experiments ($\sim 10^7$ cells ml^{-1}), naphthalene concentrations of 40 to 100 ng ml^{-1} were insufficient to support growth, thus validating the use of first-order Michaelis-Menten kinetic models (32). Furthermore, we observed similar biodegradation kinetics in experiments in which chloramphenicol was added at a concentration (34 μg ml^{-1}) previously found to inhibit cell division.

When Colwood soil slurries (0 to 200 mg ml^{-1}) preequilibrated (25 days) with a constant initial mass of naphthalene were inoculated with NP-Alk at a density of (0.57 ± 0.08) $\times 10^7$ cells ml^{-1}, dramatic reductions in both the rates and extents of naphthalene mineralization at increasing soil concentrations (and thus decreasing aqueous-phase naphthalene concentrations) were observed in mineralization assays (Fig. 1a). Similar results were observed in mineralization assays using Oshtemo soil as the sorbent after 6 days of equilibration and a cell density of (1.18 ± 0.14) $\times 10^7$ cells ml^{-1} (Fig. 1b). Initial mineralization rates derived from the first-order mineralization rate constants (equation 1) were directly proportional to the equilibrium aqueous-phase naphthalene concentrations and fell below the theoretical lines connecting the soil-free control rates to the origins (Fig. 2a and b). These data show clearly that naphthalene mineralization rates were limited by the concentrations of dissolved substrate.

Sorption also limited the extent to which naphthalene was degraded by NP-Alk (Fig. 1). Figure 3 shows the general decrease in P_{max} values with decreasing equilibrium aqueous-phase naphthalene concentrations resulting from sorption. The data points for Colwood soil slurries (Fig. 3a) fell somewhat above the theoretical line, indicating that a portion of the sorbed naphthalene was mineralized. However, this naphthalene did not effect increases in initial mineralization rates (Fig. 2a), indicating that it became available slowly over the course of the assay. The data for Oshtemo soil slurries (Fig. 3b) were closely scattered around the theoretical line, indicating that desorption rates were slow relative to biodegradation rates and that sorbed naphthalene was not utilized by the cells during the assay.

Fitting of the data for NP-Alk to the coupled degradation-desorption model (equation 3) resulted in parameter estimates which agreed well with the simple first-order model (equation 1) (Fig. 2 and 3 and Table 2). First-order rate constants (ks), initial mineralization rates (v_1[naphthalene]$_{init}$), and extents of mineralization (v_1/k) approximated their equivalent values {k,$k(P_{max})$[naphthalene]$_{init}$, and P_{max},

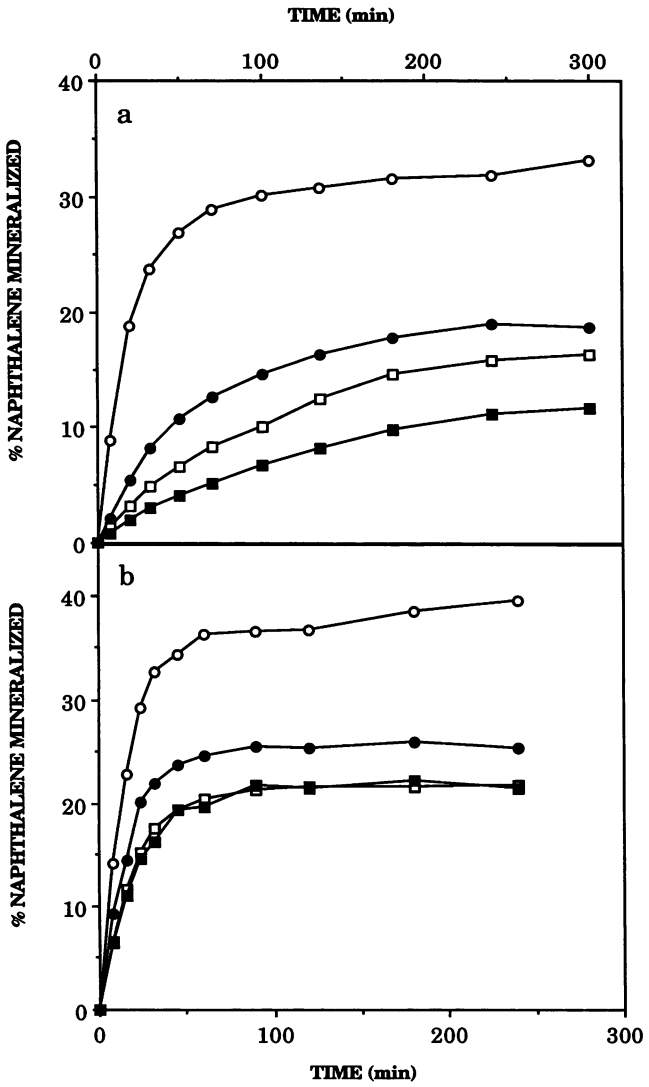

FIG. 1. Naphthalene mineralization time courses for NP-Alk in soil-free controls (○) and Colwood (a) and Oshtemo (b) soil slurries containing 66.7 (●), 133.3 (□), or 200 (■) mg of soil ml^{-1}.

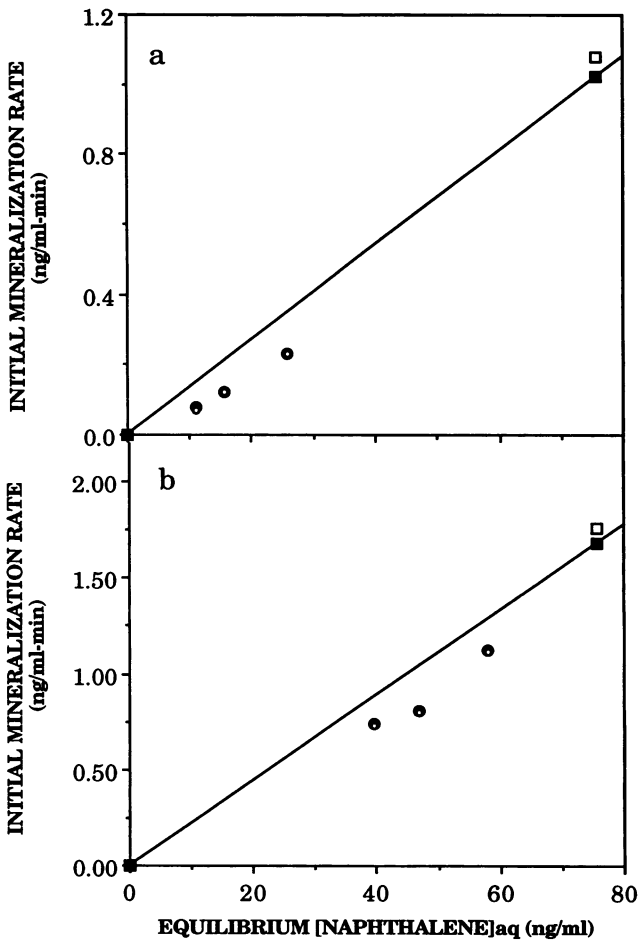

FIG. 2. Plots of initial mineralization rates for NP-Alk versus the equilibrium aqueous-phase naphthalene concentrations for the Colwood (a) and Oshtemo (b) data in Fig. 1. For both soils, the rates (estimated by using equation 1) in slurries (●) fell below the theoretical lines connecting the soil-free controls (■) with the origin. Initial mineralization rates obtained by using the coupled degradation-desorption model are also shown (open symbols).

respectively} obtained with the first-order model. Values of v_2 were low relative to v_1, confirming that desorption did not contribute significantly to the naphthalene mineralization observed. The coupled degradation-desorption model, while providing somewhat lower residual sums of squares (RSS), essentially degenerated to the first-order model when used to fit mineralization data for NP-Alk.

Similar experiments with *P. putida* 17484 yielded different results. With the Capac and Colwood soils as naphthalene sorbents, pre-equilibrated (2 days) slurries at various soil-solution ratios (0 to 192 mg ml^{-1}) were inoculated with strain 17484 at a density of 0.71×10^7 cells ml^{-1}. Figure 4 shows the mineralization time courses for a soil-free control and soil-water suspensions at three concentrations of the Capac and Colwood soils. Mineralization was rapid and extensive in all of the systems. Mineralization curves, particularly at high sorbent levels, showed pronounced deviations from simple first-order kinetics, with a rapid exponential phase followed by a linear phase of $^{14}CO_2$ production.

Fitting of the data for strain 17484 to the first-order model (equation 1) resulted in high RSS (Table 3). Significant (F test at the 0.005 level) reductions in RSS were obtained when data for soil slurries were fitted to the coupled degradation-desorption model (equation 3). Theoretical curves for the two soils at a soil concentration of 192 mg ml^{-1} show the excellent fits provided by the three-parameter model (Fig. 5, dashed lines).

When initial mineralization rates ($v_1[\text{naphthalene}]_{init}$) in bioavailability assays with strain 17484 were plotted as a function of the equilibrium aqueous-phase naphthalene concentration, all data fell well above the theoretical line (Fig. 6a). These data show that mineralization by strain 17484 was not limited to solution phase naphthalene but that a significant portion of the sorbed naphthalene was also directly available to this organism. Similar trends were consistently observed when initial mineralization rates obtained by using the first-order model were plotted, because of the combined underestimation of k and overestimation of the asymptote of the exponential reaction (P_{max}) which this model generated in attempting to fit the data. This model also indicated that

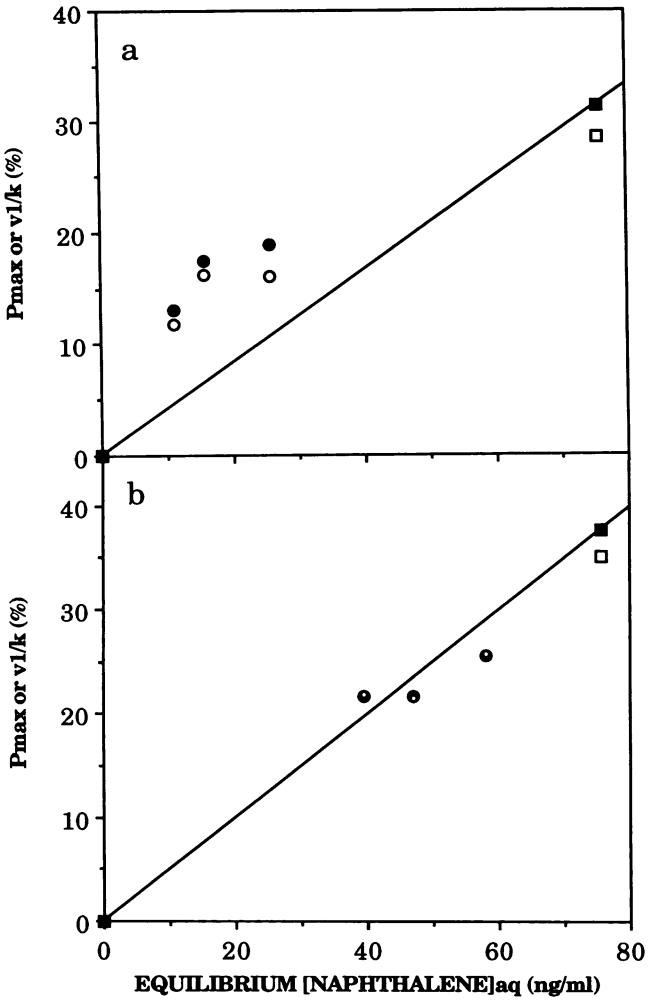

FIG. 3. Plots of P_{max} for NP-Alk versus the equilibrium aqueous-phase naphthalene concentrations for the Colwood (a) and Oshtemo (b) data in Fig. 1. P_{max} values in slurries (●) generally decreased with decreasing aqueous-phase naphthalene concentrations, with some scatter around the theoretical lines connecting the soil-free P_{max} values (■) to the origin. Extents of mineralization (v_1/k) obtained by using the coupled degradation-desorption model are also shown (open symbols).

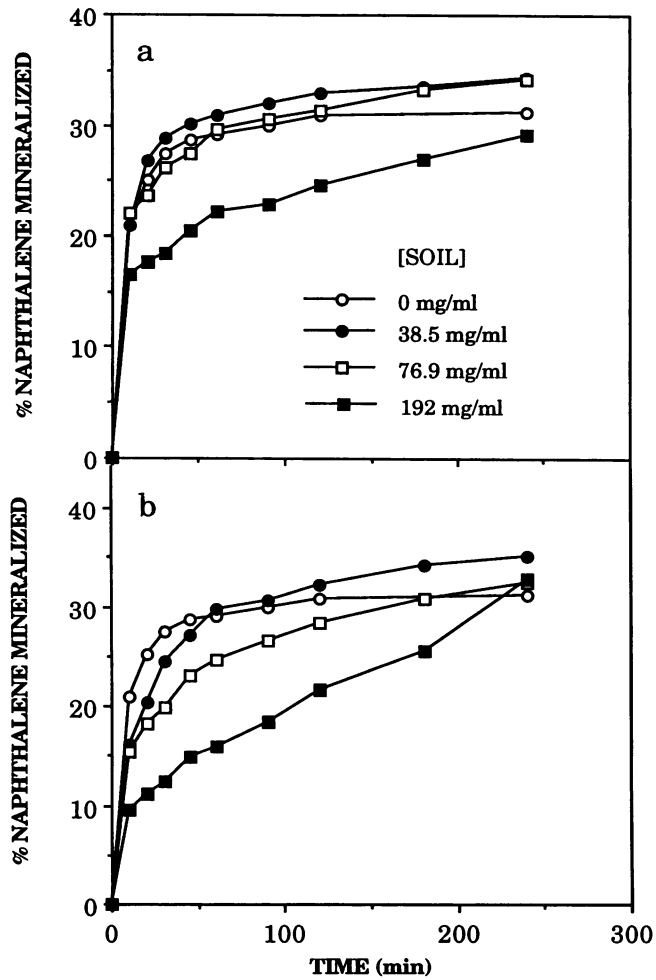

FIG. 4. Naphthalene mineralization time courses for strain 17484 in a soil-free control and Capac (a) and Colwood (b) soil slurries. Soil concentrations in panel b are the same as those indicated by the symbols in panel a.

the extent of naphthalene mineralization by strain 17484 in soil slurries (P_{max}) was largely independent of the equilibrium aqueous-phase naphthalene concentration (Table 3).

The P_{max} equivalents obtained by using the coupled degradation-desorption model (v_1/k) consistently and significantly exceeded the theoretical values predicted from the equilibrium aqueous-phase naphthalene concentration (Fig. 6b). This indicates that strain 17484 had direct and immediate access to a significant fraction of the sorbed naphthalene in slurries. In contrast to NP-Alk, P_{max} (or v_1/k) values above the predicted values supported initial mineralization rates which exceeded the theoretical rates for strain 17484 (Fig. 6a).

Estimates of v_2 in experiments with strain 17484 were considerably higher than in experiments with NP-Alk (Tables 2 and 3), indicating very different behavior of sorbed naphthalene in bioavailability experiments with the two organisms. Mineralization curves showed that strain 17484 was able to mineralize essentially all of the naphthalene in slurries over the 4- or 5-h time course of the assays (Fig. 4), whereas sorbed naphthalene in experiments with NP-Alk remained largely unavailable (Fig. 1).

For strain 17484, v_2 (the rate of mineralization associated with desorption of bound naphthalene) increased as the equilibrium aqueous-phase naphthalene concentration decreased (Fig. 6c). It should be mentioned here that with increasing sorbent concentrations and a constant initial mass of naphthalene, the actual naphthalene concentrations in both the solution and sorbed phases decreased. This implies that strain 17484 was more effective in facilitating desorption of bound naphthalene when it was more highly dispersed over the sorbent mass, although such dispersion limited the accessibility (v_1/k) of the sorbed naphthalene in the short term (Fig. 6b). For both strain 17484 and NP-Alk, estimates of v_2 in soil-free controls were greater than zero, indicating the limitations of the model in distinguishing slow desorption rates from experimental noise.

As a summary comparison of the two organisms, initial mineralization rates determined with the coupled degradation-desorption model in bioavailability experiments con-

TABLE 2. Parameter estimates and calculated rates and extents of naphthalene mineralization based on the simple first-order model and the coupled degradation-desorption model for the NP-Alk bioavailability data in Fig. 1

[Soil][a]	First-order model				Coupled degradation-desorption model					
	P_{max}	k	RSS	Rate[b]	v_i	v_2	k	RSS	Rate[b]	v_1/k
Colwood										
0	31.362 (0.353)[c]	0.043 (0.002)	6.530	1.02	1.424 (0.017)	0.013 (0.002)	0.050 (0.001)	0.945[d]	1.08	28.48
66.7	18.840 (0.251)	0.016 (0.001)	1.218	0.23	0.305 (0.009)	0.008 (0.004)	0.019 (0.002)	0.876[e]	0.23	16.05
133.3	17.488 (0.302)	0.009 (0.000)	0.584	0.12	0.162 (0.011)	0.001 (0.007)	0.010 (0.001)	0.583[e]	0.12	16.20
200	13.075 (0.243)	0.008 (0.000)	0.208	0.08	0.095 (0.013)	0.002 (0.008)	0.008 (0.002)	0.206[e]	0.07	11.88
Oshtemo										
0	37.743 (0.410)	0.059 (0.003)	7.285	1.68	2.327 (0.066)	0.015 (0.004)	0.066 (0.003)	2.648[d]	1.76	35.25
66.7	25.588 (0.221)	0.058 (0.002)	2.096	1.12	1.472 (0.004)	−0.001 (0.004)	0.057 (0.003)	2.071[e]	1.11	25.82
133.3	21.709 (0.069)	0.049 (0.001)	0.423	0.80	1.058 (0.018)	0.000 (0.002)	0.049 (0.001)	0.423[e]	0.80	21.59
200	21.769 (0.185)	0.045 (0.002)	1.418	0.74	0.966 (0.028)	−0.001 (0.004)	0.044 (0.002)	1.388[e]	0.73	21.95

[a] Soil concentrations are in milligrams (dry weight) milliliter^{-1}.
[b] Initial mineralization rates as defined in the text.
[c] Values in parentheses are standard deviations of parameter estimates.
[d] Reduction in RSS significant at the 0.01 confidence level.
[e] Reduction in RSS insignificant at the 0.1 confidence level.

ducted over a 1-year period were examined. To facilitate comparison of these data in which equilibration times and cell densities varied, a rate enhancement factor was calculated as follows: rate enhancement factor = ([initial mineralization rate]$_{slurry}$/[initial mineralization rate]$_{control}$)/(equilibrium aqueous-phase [naphthalene]$_{slurry}$/[naphthalene]$_{control}$). A rate enhancement factor of unity is expected in the hypothetical case in which only dissolved naphthalene is available. Figure 7 shows that measured rates for NP-Alk were consistently lower than the theoretical rates and decreased monotonically with decreasing equilibrium aqueous-phase naphthalene concentrations. For strain 17484, rates increased with decreasing equilibrium aqueous-phase naphthalene concentrations with rate enhancement factors up to 4.5 times the theoretical rate factor at high sorbent levels. This suggests that strain 17484 is highly efficient in utilizing sorbed naphthalene.

DISCUSSION

The influence of sorption on the bioavailability of naphthalene in soils varies with the degradative organism in question. Whereas sorption generally acts to decrease the rate of naphthalene mineralization relative to soil-free systems containing the same mass of naphthalene, the magnitude of this effect is highly organism specific because of the differential bioavailability of sorbed naphthalene to bacteria. Here we have described a simple kinetic approach for assessment of whether, and to what extent, sorbed naphthalene is available to potential microbial degraders. Although it requires accurate estimates of Michaelis-Menten kinetic constants for naphthalene utilization by the organisms, this approach makes examination of individual experimental variables (sorption coefficient, NOC solubility, solute-sorbent aging, bacterial motility, etc.) possible.

For the soil isolate, NP-Alk, sorbed naphthalene was relatively unavailable, as shown by the initial mineralization rates in soil slurries as a function of the equilibrium aqueous-phase naphthalene concentration. Analysis of P_{max} and v_1/k data also indicated that this organism was relatively ineffective in gaining access to sorbed naphthalene, although slow desorption of bound naphthalene supported some additional mineralization (see below).

Sorbed naphthalene was directly available to *P. putida* 17484, inasmuch as initial mineralization rates in soil slurries

TABLE 3. Parameter estimates and calculated rates and extents of naphthalene mineralization based on the simple first-order model and the coupled degradation-desorption model for the strain 17484 bioavailability data in Fig. 4

[Soil][a]	First-order model				Coupled degradation-desorption model					
	P_{max}	k	RSS	Rate[b]	v_1	v_2	k	RSS	Rate[b]	v_1/k
0	29.805 (0.586)[c]	0.102 (0.015)	7.970	1.55	3.486 (0.433)	0.015 (0.004)	0.125 (0.018)	3.437[d]	1.78	27.89
Capac										
38.5	32.309 (0.550)	0.089 (0.008)	14.195	1.47	3.389 (0.143)	0.022 (0.002)	0.116 (0.005)	1.753[e]	1.73	29.22
76.9	30.896 (1.10)	0.086 (0.019)	50.225	1.35	4.117 (0.661)	0.039 (0.007)	0.160 (0.029)	10.823[e]	2.10	25.73
192	24.582 (1.321)	0.065 (0.021)	67.992	0.81	3.742 (0.884)	0.049 (0.005)	0.211 (0.053)	5.140[e]	1.91	17.73
Colwood										
38.5	32.653 (1.146)	0.048 (0.004)	26.718	0.80	1.907 (0.182)	0.035 (0.007)	0.071 (0.009)	8.586[e]	0.97	26.86
76.9	29.000 (1.320)	0.044 (0.003)	54.491	0.65	2.092 (0.244)	0.052 (0.006)	0.102 (0.014)	10.833[e]	1.07	20.51
192	29.449 (3.421)	0.015 (0.004)	85.239	0.22	1.800 (0.478)	0.093 (0.003)	0.189 (0.052)	2.687[e]	0.92	9.52

[a] Soil concentrations are in milligrams (dry weight) milliliter^{-1}.
[b] Initial mineralization rates as defined in the text.
[c] Values in parentheses are standard deviations of parameter estimates.
[d] Reduction in RSS significant at the 0.025 confidence level.
[e] Reduction in RSS significant at the 0.005 confidence level.

consistently exceeded the rates expected if only dissolved substrate were available. These rates indicated that the average cell had access to high localized naphthalene concentrations such as those that might occur at the sorbent-water interface. Direct access to sorbed naphthalene phases was also evidenced by the v_1/k values, which exceeded theoretical values. The physical form in which this excess naphthalene is available to strain 17484 is unknown. We have noted, however, that this organism is chemotactic toward naphthalene and attaches reversibly to soils, whereas NP-Alk attaches more extensively and irreversibly (13).

To explain the kinetics of NOC interactions with soils, the two-compartment mass transfer model of sorption-desorption processes was developed by Karickhoff (15). With increasing equilibration time, soil organic carbon, or solute hydrophobicity, NOCs partition increasingly from the aqueous phase to a labile sorbed phase and ultimately to a nonlabile sorbed phase. Because the mass transfer rate constants defining movement between the labile and nonlabile phases are much slower than those that define movement between the labile sorbed and dissolved phases, the disposition of solute within the two sorbent phases would be expected to result in different degrees of availability and rates of desorption. Direct access to surface-localized, labile sorbed naphthalene by strain 17484 is a reasonable interpretation of the data, consistent with the model of Karickhoff. Such utilization might then be responsible for the rapid desorption (or outward diffusion) of nonlabile sorbed naphthalene, giving rise to the high values of v_2 observed for this organism.

Few studies have attempted a quantitative kinetic analysis of the influence of sorption on biodegradation without assuming that equilibrium or pseudoequilibrium conditions exists. Ogram et al. (24) modeled 2,4-D degradation in soils by assuming instantaneous equilibrium and complete desorption and using the simple first-order model (equation 1) used here but setting P_{max} equal to 100% for slurries and soil-free controls alike. By treating P_{max} as a variable parameter to be estimated in equation 1, we could assess the effect of sorption on the extent of naphthalene degradation in soils. This model worked well under the pseudoequilibrium condition, in which the rate of biodegradation was much faster than the rate of desorption. This was the case for NP-Alk, for which v_2 was small relative to v_1 (Table 2), and the extent of degradation (P_{max} or v_1/k) approximated the values predicted on the basis of the equilibrium aqueous-phase naphthalene concentrations (Fig. 3).

When desorption rates are of the same order as biodegradation rates, nonequilibrium conditions prevail. Few models have been put forth to describe the kinetics of substrate mineralization under nonequilibrium conditions. To develop even the simplest model on theoretical grounds would require inclusion (or a priori knowledge) of physical parameters (or variables) such as the proportion of sorbed solute residing in dissolved and labile and nonlabile sorbed phases, the kinetics of mass transfer between the phases, the duration of sorbate-sorbent contact, etc. To develop more complex models, in which desorption is assumed to be governed by radial diffusion, detailed knowledge about aggregate size, intra-aggregate pore structure, and additional variables (or model parameters) is required. In addition to physical variables, biological parameters, such as bacterial attachment to the sorbent, would also be components of such models. With increased parameterization of models comes the increased difficulty of being able to estimate all of the parameters uniquely.

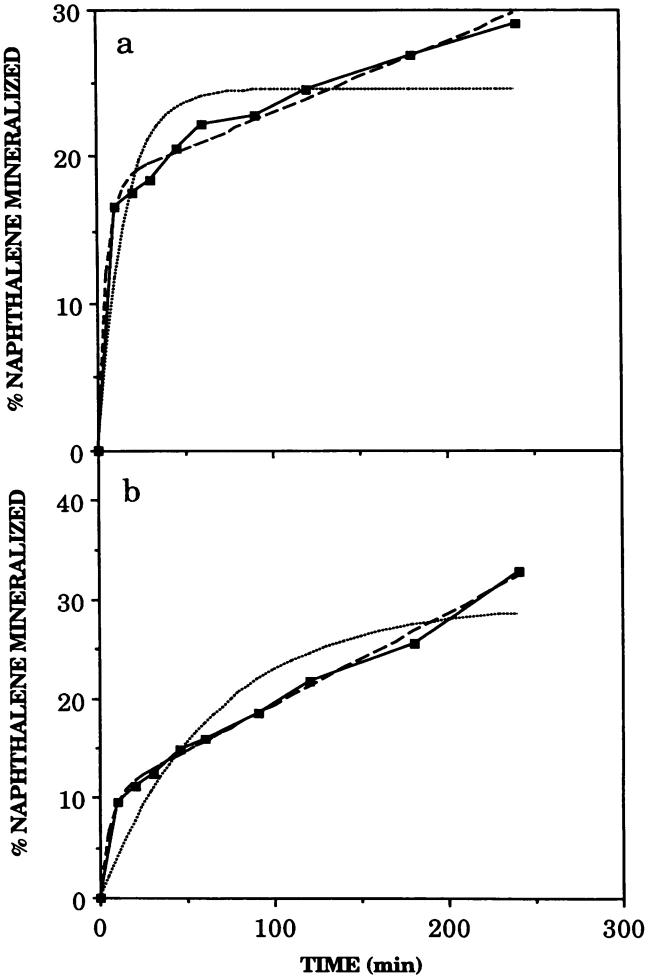

FIG. 5. Theoretical curves generated by using the parameter estimates obtained with the simple first-order model (equation 1; dotted lines) and the coupled degradation-desorption model (equation 3; dashed lines) for the Capac (192 mg ml^{-1}) (a) and Colwood (192 mg ml^{-1}) (b) soil slurry data shown in Fig. 4 for strain 17484. The actual datum points are connected by solid lines.

Here we found empirically that a simple three-parameter model provided excellent fits to experimental data in systems not at equilibrium. The model degenerated to the simple first-order model (nested within it) as the systems approximated equilibrium conditions. The simplicity of the coupled degradation-desorption model offers a reasonable first attempt to examine the kinetics of naphthalene mineralization under nonequilibrium conditions. F tests showed highly significant (0.005 confidence level) reductions in RSS for strain 17484 data in slurries with this model as opposed to the simple first-order model. For NP-Alk, RSS reductions using the coupled degradation-desorption model for slurry data were insignificant.

In addition to describing the mineralization kinetics of immediately accessible naphthalene, and the size of this pool, the coupled degradation-desorption model also provides information about the rate of naphthalene desorption from the soil. By normalizing the v_2 values obtained with this model to the fraction of naphthalene sorbed (v_2/fraction of naphthalene sorbed), pseudo-first-order desorption rate con-

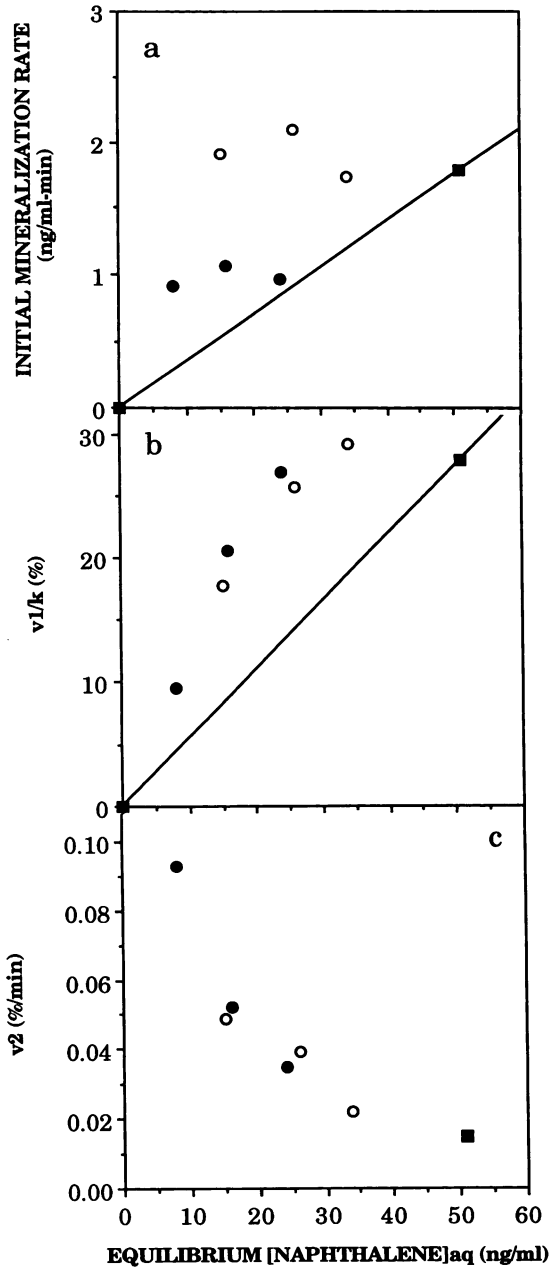

FIG. 6. Plots of initial mineralization rates (a), sizes of the immediately accessible naphthalene pools (b), and rates of mineralization due to desorption (c) versus equilibrium aqueous-phase naphthalene concentrations for the Capac (○) and Colwood (●) bioavailability data shown in Fig. 4 for strain 17484 and calculated by using the coupled degradation-desorption model. In panels a and b, all points fall above the theoretical lines connecting the soil-free control datum points (solid squares) to the origins, indicating that sorbed naphthalene is directly available to this organism. In panel c, v_2 values increase with increasing sorption (lower equilibrium aqueous-phase concentrations) of naphthalene. The solid square in panel c is the v_2 value for the soil-free control.

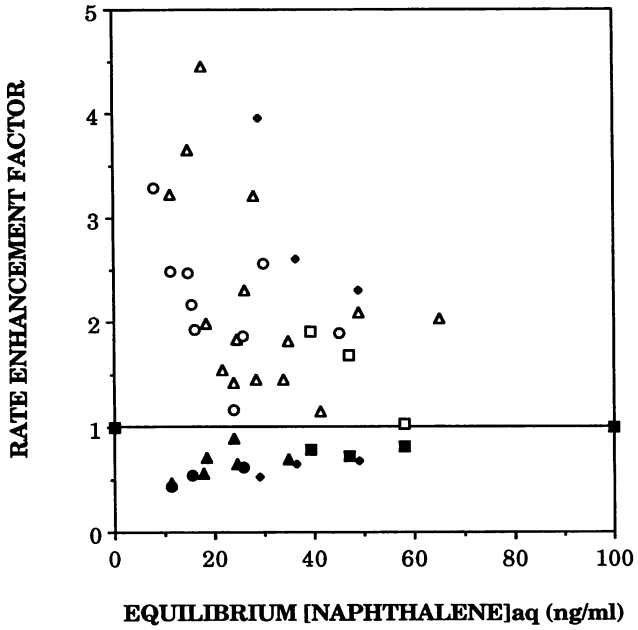

FIG. 7. Summary comparison of the influence of sorption on naphthalene mineralization by strain 17484 (open symbols) and NP-Alk (solid symbols). Rate enhancement factors (defined in the text) are plotted versus the equilibrium aqueous-phase naphthalene concentrations for bioavailability experiments conducted over a 1-year period with Capac (triangles), Colwood (circles), Oshtemo (squares), and Schoolcraft (diamonds) soils as the sorbents.

stants can be obtained. Despite variable v_2 values for strain 17484 in soil slurries (Fig. 6c), this normalization yielded an average pseudo-first-order desorption rate constant of 0.047 h^{-1} (± 0.010, n = 6). Similar treatment of data for NP-Alk from bioavailability experiments with the Capac, Colwood, and Schoolcraft soils (but not the Oshtemo data shown here, for which v_2 was statistically zero) as sorbents gave an average value of 0.007 ± 0.005 h^{-1} (n = 12). Thus, strain 17484 effects a sevenfold enhancement of naphthalene desorption from soil in comparison with NP-Alk. Although not accounting for incorporation of naphthalene into biomass causes two- or threefold underestimation of these constants, they are at least an order of magnitude smaller than the first-order desorption rate constants (mass transfer from nonlabile to labile sorbed phase) for naphthalene from river sediments (0.49 to 0.94 h^{-1}) measured by Karickhoff (15) in abiotic systems by using a gas purge technique. Nevertheless, we propose that by directly mineralizing surface-localized, labile sorbed naphthalene, strain 17484 establishes steep concentration gradients to promote desorptive diffusion and mineralization of nonlabile naphthalene partitioned in the interior of soil organic particles. Conversely, it appears that NP-Alk relies on the passive desorption of bound naphthalene to support mineralization.

The kinetic analyses reported here refer to the average activities of the cells in bioavailability assays. In their study, Ogram et al. (24) found that free-living and attached cells of a *Flavobacterium* sp. mineralized dissolved 2,4-D with approximately equal efficiencies, while soil-sorbed 2,4-D was unavailable to all cells. In different sorbate-sorbent systems, disposition of the degrading cells with respect to the sorbent was of paramount importance in determining degradation. Kefford et al. (16) reported vastly different scavenging efficiencies of stearic acid coated on glass depending on the mode of interaction of three different bacterial strains with the coated surface. Pigmented wild-type *Serratia* sp. attached irreversibly to the glass and mineralized the stearate

to a much greater extent than the free-living, nonpigmented mutant. A gliding *Leptospira* sp. was the most active scavenger of sorbed stearate because of its ability to contact the sorbent and actively seek new substrate sources once the substrate was depleted in a particular area. Similarly, Griffith and Fletcher (11) reported more efficient use of sorbed protein by an attached *Pseudomonas* sp., while the unattached mutant was more efficient at mineralizing a nonsorbing, fluorescently tagged dipeptide. This is the first report of the differential availability of a sorbed NOC to two bacterial species. The underlying basis of the observed differences is under investigation.

ACKNOWLEDGMENTS

We acknowledge helpful discussions with J. Robinson on the modeling aspects of this work and the technical assistance of J. Marks.

This work was supported by grant DE-FGO2-89ER60809 from the U.S. Department of Energy, Subsurface Science Program, and the Michigan Agricultural Experiment Station.

REFERENCES

1. **Abdul, A. S., T. L. Gibson, and D. N. Rai.** 1987. Statistical correlations for predicting the partition coefficient for nonpolar organic contaminants between aquifer organic carbon and water. Hazard Waste Hazard Mater. **4:**211–222.
2. **Alexander, M., and K. M. Scow.** 1989. Kinetics of biodegradation in soil, p. 243–269. *In* B. L. Sawhney and K. Brown (ed.), Reactions and movement of organic chemicals in soil. Soil Science Society of America special publication no. 22. Soil Science Society of America, Madison, Wis.
3. **Ball, W. P., and P. V. Roberts.** 1991. Long-term sorption of halogenated organic chemicals by aquifer material. 2. Intraparticle diffusion. Environ. Sci. Technol. **25:**1237–1249.
4. **Barnsley, E. A.** 1976. Role and regulation of the *ortho* and *meta* pathways of catechol metabolism in pseudomonads metabolizing naphthalene and salicylate. J. Bacteriol. **125:**404–408.
5. **Brunner, W., and D. D. Focht.** 1984. Deterministic three-half-order kinetic model for microbial degradation of added carbon substrates in soil. Appl. Environ. Microbiol. **47:**167–172.
6. **Brusseau, M. L., R. E. Jessup, and P. S. C. Rao.** 1991. Nonequilibrium sorption of organic chemicals: elucidation of rate-limiting processes. Environ. Sci. Technol. **25:**134–142.
7. **Chiou, C. T., L. J. Peters, and V. H. Freed.** 1979. A physical concept of soil-water equilibria for nonionic organic compounds. Science **206:**831–832.
8. **Connors, M. A., and E. A. Barnsley.** 1982. Naphthalene plasmids in pseudomonads. J. Bacteriol. **149:**1096–1101.
9. **Fletcher, M.** 1985. Effect of solid surfaces on the activity of attached bacteria, p. 339–362. *In* D. C. Savage and M. Fletcher (ed.), Bacterial adhesion. Plenum Press, New York.
10. **Gordon, A. S., and F. J. Millero.** 1985. Adsorption mediated decrease in the biodegradation rate of organic compounds. Microb. Ecol. **11:**289–298.
11. **Griffith, P. C., and M. Fletcher.** 1991. Hydrolysis of protein and model dipeptide substrates by attached and nonattached marine *Pseudomonas* sp. strain NCIMB 2021. Appl. Environ. Microbiol. **57:**2186–2191.
12. **Grigal, D. F.** 1973. Note on the hydrometer method of particle-size analysis. Minnesota Forestry Research Notes, no. 245. University of Minnesota, St. Paul.
13. **Guerin, W. F., and S. A. Boyd.** Unpublished data.
14. **Guerin, W. F., and G. E. Jones.** 1988. Two-stage mineralization of phenanthrene by estuarine enrichment cultures. Appl. Environ. Microbiol. **54:**929–936.
15. **Karickhoff, S. W.** 1980. Sorption kinetics of hydrophobic pollutants in natural sediments, p. 193–205. *In* R. A. Baker (ed.), Contaminants and sediments, vol. 2. Ann Arbor Science, Ann Arbor, Mich.
16. **Kefford, B., S. Kjelleberg, and K. C. Marshall.** 1982. Bacterial scavenging: utilization of fatty acids localized at a solid-liquid interface. Arch. Microbiol. **133:**257–260.
17. **Kiyohara, H., and K. Nagao.** 1978. The catabolism of phenanthrene and naphthalene by bacteria. J. Gen. Microbiol. **105:**69–75.
18. **Lao, R. C., R. S. Thomas, and J. L. Monkman.** 1975. Computerized gas chromatographic-mass spectrometric analysis of polycyclic aromatic hydrocarbons in environmental samples. J. Chromatogr. **112:**681–700.
19. **Larson, R. J.** 1980. Environmental extrapolation of biotransformation data. Role of biodegradation kinetics in predicting environmental fate, p. 67–86. *In* A. W. Maki, K. L. Dickson, and J. Cairns, Jr. (ed.), Biotransformation and fate of chemicals in the aquatic environment. American Society for Microbiology, Washington, D.C.
20. **Larson, R. J.** 1984. Kinetic and ecological approaches for predicting biodegradation rates of xenobiotic organic chemicals in natural ecosystems, p. 677–686. *In* M. J. Klug and C. A. Reddy (ed.), Current perspectives in microbial ecology. American Society for Microbiology, Washington, D.C.
21. **Leatherbarrow, R. J.** 1990. Using linear and non-linear regression to fit biochemical data. Trends Biochem. Sci. **15:**455–458.
22. **Marshall, K. C.** 1976. Interfaces in microbial ecology. Harvard University Press, Cambridge, Mass.
23. **May, W. E., S. P. Wasik, and D. H. Freeman.** 1978. Determination of the solubility behavior of some polycyclic aromatic hydrocarbons in water. Anal. Chem. **50:**997–1000.
24. **Ogram, A. V., R. E. Jessup, L. T. Lou, and P. S. C. Rao.** 1985. Effects of sorption on biological degradation rates of (2,4-dichlorophenoxy)acetic acid in soils. Appl. Environ. Microbiol. **49:**582–587.
25. **Readman, J. W., R. F. C. Mantoura, M. M. Rhead, and L. Brown.** 1982. Aquatic distribution and heterotrophic degradation of polycyclic aromatic hydrocarbons (PAH) in the Tamar Estuary. Estuarine Coastal Shelf Sci. **14:**369–389.
26. **Rhoades, J. D.** 1982. Cation exchange capacity, p. 149–157. *In* A. L. Page, R. H. Miller, and D. R. Keeney (ed.), Methods of soil analysis, part 2. American Society of Agronomy, Madison, Wis.
27. **Rijnaarts, H. H. M., A. Bachmann, J. C. Jumelet, and A. J. B. Zehnder.** 1990. Effect of desorption and intraparticle mass transfer on the aerobic biomineralization of α-hexachlorocyclohexane in a contaminated calcareous soil. Environ. Sci. Technol. **24:**1349–1354.
28. **Robinson, J. A.** 1985. Determining microbial kinetic parameters using nonlinear regression analysis. Adv. Microb. Ecol. **8:**61–114.
29. **Schell, M. A.** 1990. Regulation of the naphthalene degradation genes of plasmid NAH7: example of a generalized positive control system in *Pseudomonas* and related bacteria, p. 165–176. *In* S. Silver, A. M. Chakrabarty, B. Iglewski, and E. Kaplan (ed.), *Pseudomonas*: biotransformations, pathogenesis, and evolving biotechnology. American Society for Microbiology, Washington, D.C.
30. **Shelton, D. R., and J. M. Tiedje.** 1984. Isolation and partial characterization of bacteria in an anaerobic consortium that mineralizes 3-chlorobenzoic acid. Appl. Environ. Microbiol. **48:**840–848.
31. **Shimp, R. J., and R. L. Young.** 1988. Availability of organic chemicals for biodegradation in settled bottom sediments. Ecotoxicol. Environ. Safety **15:**31–45.
32. **Simkins, S., and M. Alexander.** 1984. Models for mineralization kinetics with the variables of substrate concentration and population density. Appl. Environ. Microbiol. **47:**1299–1306.
33. **Steen, W. C., D. F. Paris, and G. L. Baughman.** 1980. Effects of sediment sorption on microbial degradation of toxic substances, p. 477–482. *In* R. A. Baker (ed.), Contaminants and sediments, vol. 1. Ann Arbor Science, Ann Arbor, Mich.
34. **Steinberg, S. M., J. J. Pignatello, and B. L. Sawhney.** 1987. Persistence of 1,2-dibromoethane in soils: entrapment in intraparticle micropores. Environ. Sci. Technol. **21:**1201–1208.
35. **van Loosdrecht, M. C. M., J. Lyklema, W. Norde, and A. J. B.**

Zehnder. 1990. Influence of interfaces on microbial activity. Microbiol. Rev. **54:**75–87.
36. **Weber, J. B., and H. D. Coble.** 1968. Microbial decomposition of diquat adsorbed on montmorillonite and kaolonite clays. J. Agric. Food Chem. **16:**475–478.
37. **Wolin, E. A., M. J. Wolin, and R. S. Wolfe.** 1963. Formation of methane by bacterial extracts. J. Biol. Chem. **238:**2882–2886.
38. **Wu, S., and P. M. Gschwend.** 1986. Sorption kinetics of hydrophobic organic compounds to natural sediments and soils. Environ. Sci. Technol. **20:**717–725.
39. **Zobell, C. E.** 1943. The effect of solid surfaces upon bacterial activity. J. Bacteriol. **46:**39–56.